# First principles study the ferromagnetic properties and electronic structure of boron doped ZnSe

**ARTICLE** *in* SOLID STATE COMMUNICATIONS · AUGUST 2012

Impact Factor: 1.9 · DOI: 10.1016/j.ssc.2012.05.025



**4 AUTHORS:**

S. W. Fan

China Three Gorges University

**32** PUBLICATIONS **226** CITATIONS

SEE PROFILE

L. J. Ding

**24** PUBLICATIONS **76** CITATIONS

SEE PROFILE

Zh. -L. Wang

**86** PUBLICATIONS **1,123** CITATIONS

SEE PROFILE

K. L. Yao

Huazhong University of Science and Techn…

**344** PUBLICATIONS **3,106** CITATIONS

SEE PROFILE

Solid State Communications 152 (2012) 1551–1555

Contents lists available at SciVerse ScienceDirect

Solid State Communications

journal homepage: www.elsevier.com/locate/ssc

# First principles study the ferromagnetic properties and electronic structure of boron doped ZnSe

S.W. Fan [a,*], L.J. Ding [a], Z.L. Wang [a], K.L. Yao [b,c]

[a] Department of Physics, China Three Gorges University, Yichang 443002, PR China
[b] School of Physics, Huazhong University of Science and Technology, Wuhan 430074, PR China
[c] International Center of Materials Physics, Chinese Academy of Science, Shenyang 110015, PR China

ARTICLE INFO

*Article history:*
Received 7 January 2012
Received in revised form
12 May 2012
Accepted 15 May 2012
by E.G. Wang
Available online 7 June 2012

*Keywords:*
A. Diluted magnetic semiconductor
D. Ferromagnetic properties
D. Electronic structure

ABSTRACT

Using the full-potential linearized augmented plane wave method with generalized gradient approximation, the magnetic properties and the electronic structure of the boron-doped ZnSe (zinc blende phase) are investigated. Spin polarization calculations show the magnetic moment of the 64-atoms supercell containing one $B_{Se}$ ($B_{Zn}$) is 3.00 (0.015) $\mu_B$. The density of states indicates the magnetic moments of the $B_{Se}$ doped configuration mainly come from the doped boron atoms and a few from its neighboring zinc atoms. The ferromagnetic and antiferromagnetic calculations for several doped configurations suggest $B_{Se}$ could induce stable ferromagnetic ground state in ZnSe hosts and ferromagnetic couplings exist between the doped boron atoms. Electronic structures show that $B_{Se}$ is p-type ferromagnetic semiconductor and hole-mediated double exchange is responsible for the ferromagnetism, while the $B_{Zn}$ doped configuration is n-type semiconductor. Relative shallow acceptor and donor levels indicate boron-doped ZnSe is ionized easily at working temperatures.



## 1. Introduction

Diluted magnetic semiconductors (DMSs) with room temperature ferromagnetism have attracted much attention for their rich physics and potential applications in spintronics and other spin-based devices [1]. During past decade, a great number of experimental works have reported the above room temperature ferromagnetism by doping the semiconductor with a small quantity of transition metal atoms, such as Cr-doped AlN [2] and ZnTe [3], TMs-doped $TiO_2$ [4,5], $In_2O_3$ [6], GaN and ZnO (see reviews, e.g., Ref. [7] and their references). Based on the electronic structure calculations, some transition metal doped DMSs have also been reported [8–10]. However, the origin of the ferromagnetism observed in transition metal doped semiconductors is still under debate. Ney et al. did not detect any ferromagnetism on the transition metal dopants by using the X-ray magnetic circular dichroism [11]. Furthermore, because of the limited solubility of transition metal impurities in particular hosts, the formation of nanoscale regions containing a large density of magnetic clusters, precipitates or ferromagnetic secondary phases have also been detected in some TM-doped DMSs [12–14], which would rule out most practical applications. To avoid the secondary magnetic phase and the magnetic ions clustering, several groups employed the intrinsic nonmagnetic and nonmetal atoms as dopants to fabricate the DMSs. Recently, the room temperature ferromagnetism for the nonmetal elements carbon doped ZnO [15,16] and $In_2O_3$ [17], boron doped ZnO [18], in which carbon substitutes for oxygen, have been reported. Moreover, several theoretical work have also predicted carbon doped CdS [19], ZnS [20,21], $TiO_2$ [22,23], nitrogen doped ZnO [24], and boron doped AlN [25] would be more promising DMSs. Up to now, few work has been focused on the magnetism and electronic structure of the boron doped ZnSe. In present work, we use the full-potential linearized augmented plane wave (FPLAPW) with the generalized gradient approximation to investigate the magnetism and electronic structure of boron-doped ZnSe. Our calculations show, when boron substitute selenium, a few percent of boron dopants could make the ZnSe be a promising DMS. The magnetic moment in 64 atoms supercell associated with one $B_{Se}$ defect is 3.00 $\mu_B$. The electronic structures show that boron-doped ZnSe is p-type ferromagnetic semiconductor and hole-mediated double exchange is responsible for the ferromagnetism.

## 2. Computational details

Calculations are performed by using the FPLAPW method with a scalar relativistic version as implemented in the WIEN2k package [26]. The generalized gradient approximation given by Perdew–Burke–Ernzerhof [27] is adopted to deal with the

* Corresponding author. Fax: +86 0717 6392370.
*E-mail address:* fansw1129@126.com (S.W. Fan).

0038-1098/$ - see front matter © 2012 Elsevier Ltd. All rights reserved.
http://dx.doi.org/10.1016/j.ssc.2012.05.025

exchange correlation potential. Based on the experimental lattice constants 5.667 Å [28], the fully relaxed $2\times2\times2$ supercells containing $B_{Se}$, $B_{Zn}$, $B_{iZn}$ and $B_{iSe}$ defects are constructed, where $B_{iZn}$ ($B_{iSe}$) means the boron atom is placed at the center of the tetrahedron formed by the nearest four zinc (selenium) atoms. The muffin-tin sphere radii of Zn, Se, and B atom are set to 2.36, 2.33 and 2.01 a.u., respectively. The basis quality, measured by the product $R_{min}K_{max}$ ($R_{min}$-minimal muffin-tin sphere radius and $K_{max}$-length of maximal reciprocal lattice vector), is set to 7.8 and the $3\times3\times3$ $k$-point meshes are used for the first Brillouin zone integration. Self-consistency is achieved when the energy difference between succeeding iterations is less than $1.0\times10^{-4}$ Ry. All the atomic positions are fully optimized until all components of the residual forces are less than 5 m Ry/bohr. To test the convergence, we increase $R_{min}K_{max}$ to 8.0 and $k$-point meshes to $4\times4\times4$ and obtain the same results.

## 3. Results and discussions

Based on the zinc blende unit cell, we construct $2\times2\times2$ supercell and use one boron atom to substitute a zinc and selenium atom, respectively. The sites of boron atom in the supercell are illustrated in Fig. 1. The positions of all the atoms in the supercell are fully relaxed. Because the radius of boron (85 pm) is much smaller than that of zinc atom (135 pm), and the electronegativity of boron (2.04) is larger than that of zinc (1.65), the geometry optimization results in the local structure around boron dopant suppressed with the selenium atoms drawn closer to the boron atom and the relaxed B–Se bond length 2.19 Å is much shorter than that of Zn–Se bond 2.454 Å. When the boron substitutes selenium, geometry optimizations lead the inward relaxation of zinc atom and a slightly shorter B–Zn bond length 2.37 Å compared to Se–Zn bond length 2.454 Å, which is mainly due to the radius of boron atom (85 pm) is a little smaller than that of selenium atom (115 pm) and the electronegativity of boron (2.04) is smaller than that of selenium (2.55) [29].

Spin-polarization calculations are performed on the above two doped configurations. The density of states for the $B_{Zn}$ doped configuration are illustrated in Fig. 2. Calculations show no clear spin splitting between the majority-spin and minority-spin channels near the Fermi level for the boron substituting the zinc case, indicating boron substituting zinc cannot induce magnetism in ZnSe hosts, which is mainly due to the doped boron atom and selenium atoms forming stable non-spin polarization covalent bonds and similar to the carbon doped ZnO [16]. The impurity bands induced by the doped boron locate near the bottom of the conductor bands, which indicated $B_{Zn}$ is n-type semiconductor. Whereas there is clear spin splitting between the majority-spin and minority-spin channels near the Fermi level for the boron (spin-polarization band structures illustrated in the Fig. 3) substituting selenium doped configuration, the asymmetric band structures near the Fermi level imply boron replacing the selenium can order magnetic moments in the ZnSe. The total magnetic moment, which is mainly from the doped boron atom, is 3.00 $\mu_B$ per supercell. The doped boron contributes 0.89 $\mu_B$ and the nearest neighboring zinc (next neighboring selenium) contributes 0.11 $\mu_B$ (0.036 $\mu_B$) per atom, respectively. Other atoms contribute a few to the magnetic moments. In addition, all the atoms in the supercell are polarized in the same direction with that of the boron, indicating there exists ferromagnetic coupling between the doped boron atoms and its neighboring (next neighboring) zinc (selenium) atoms. The majority-spin channel keeps 0.80 eV energy gap, while the minority-spin channel keeps 1.20 eV energy gap. The spin-splitting impurity states leaded by the boron dopants locate between the highest occupied molecular orbital and the Fermi level in the major spin channels, implying that boron-doped ZnSe with 3.25% doped concentration is a typical p-type ferromagnetic semiconductor. Such shallow acceptor levels indicate boron-doped ZnSe is ionized easily at room temperature, which would give rise to the charge carriers within the impurity states mobile sufficiently and benefit the conductivity and the magnetic coupling.

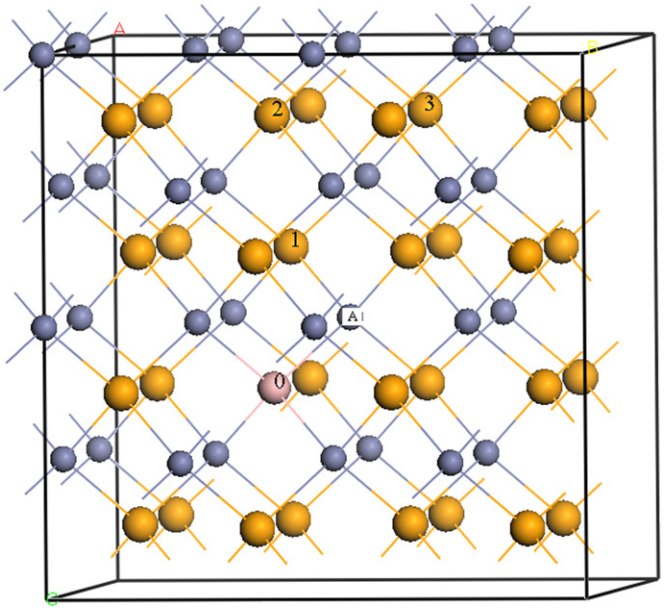


**Fig. 1.** (Color online) The supercell is used in the calculation. Yellow (gray) balls indicate selenium (Zinc) atom. The positions of selenium substituted by boron are denoted by 0 and 1–3, and the site of zinc replaced by boron is denoted by A.

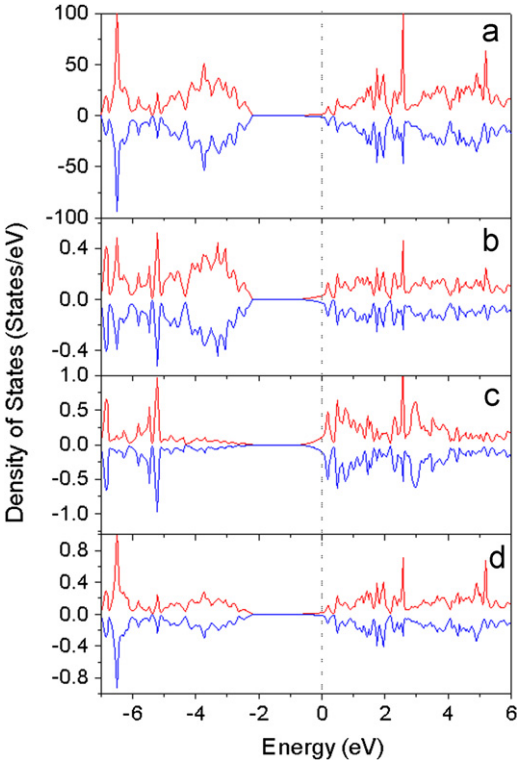


**Fig. 2.** (Color online) The total DOS for $B_{Zn}$ doped configuration is shown in (a). The (b)–(d) show the DOS for the selenium, boron and zinc state, respectively. The blue and red lines represent the majority and minority spin, respectively. Fermi level is set to 0 eV and indicated by the dotted vertical line.

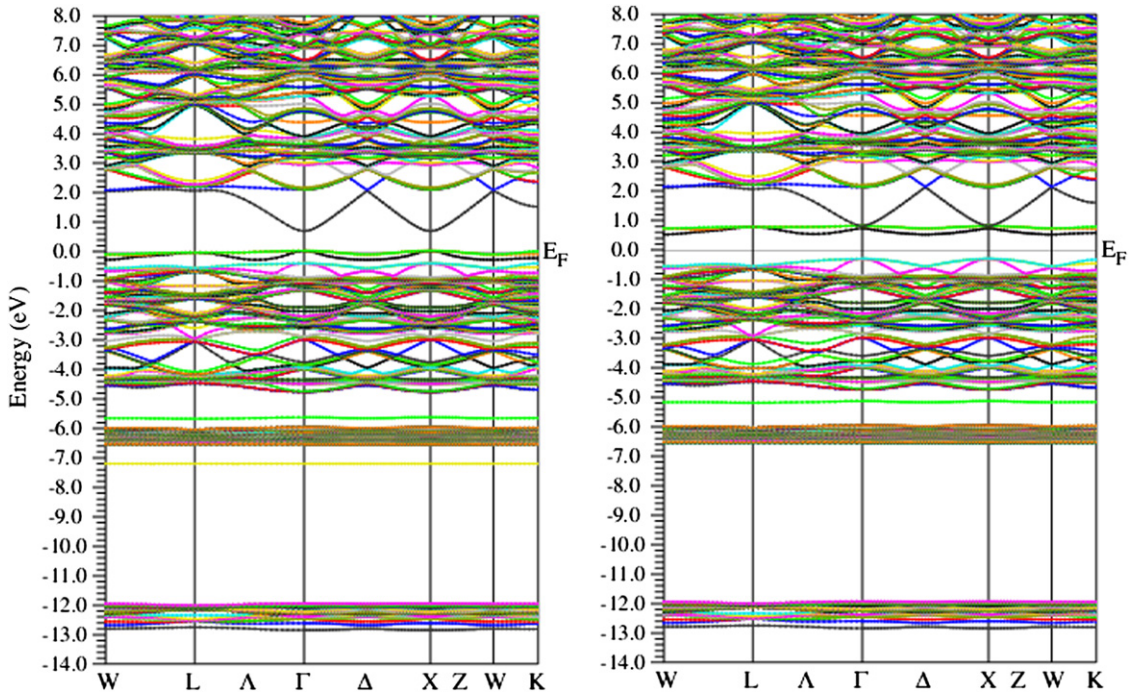


**Fig. 3.** (Color online) The band structures for $B_{Se}$ doped configuration are plotted. The left (right) represent the spin majority (minority) channel, respectively. Fermi level is indicated by the horizontal line and labeled by $E_F$.

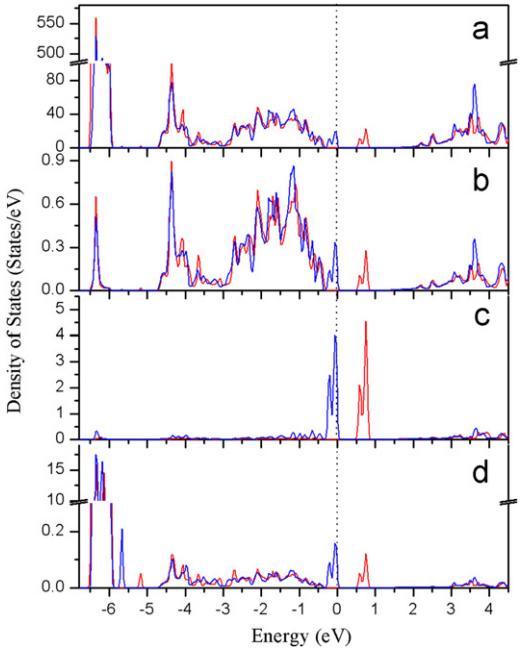


**Fig. 4.** (Color online) The total DOS for $B_{Se}$ doped configuration is shown in (a). The (b)–(d) show the partial DOS for the boron-2p, zinc-3d, and selenium-4p state, respectively. The blue and red lines represent the majority and minority spin, respectively. Fermi level is set to 0 eV and indicated by the dotted vertical line.

To investigate the origin of the magnetic moments, we calculate the spin-polarization total density of states (DOS) (shown in the Fig. 4 (a)) for the $B_{Se}$ doped configuration. Our calculations show the impurities bands reside in the energy gap and the total DOS of the majority and minority-spins are significantly splitting near the Fermi level. Below the Fermi level, there is a peak in the majority-spin channel while no states stay at the minority-spin bands. Some localized unoccupied bands exist above the Fermi level while majority-spin states are absent in this energy interval. The asymmetrical DOS between the majority and minority spin channels near the Fermi level suggests the magnetism of such doped system. To analyze the components of the impurity bands, the partial density of states (PDOS) of boron atom and its neighboring zinc (next neighboring selenium) atoms are calculated and plotted in the Fig. 4(a)–(d). The PDOS show the impurity bands are mainly from the 2p-orbital of the boron, while a few come from the 3d-orbital of the neighboring zinc and 4p-orbital of the next neighboring selenium atoms. The PDOS indicate there is strong coupling between the 2p-orbitals of boron atoms and 3d-orbitals of zinc, 4p-orbitals of selenium near the Fermi level. The PDOS of 2p-orbitals of the boron atom indicate the magnetic moments mainly contributed by the boron-2p orbital, which is similar to that of boron-doped AlN [25] and CdS [30]. The Zn-3d levels mainly locate below Fermi level by more than 5.0 eV; therefore, the $Zn^{2+}$ ion is chemically inactive. The impurity states are determined by the interaction between the dopant atomic states and the host states, the interaction of the atomic states with the valence band or conduction band would form bonding or antibonding states [30]. Due to the electronegativity of boron is less than that of selenium, it interacts less with the host atoms and the antibonding (bonding) states interacted with the conduction band (valence band) could not be pulled up (pushed down ) to the conduction band (valence band), resulting in the impurity states located in the band gap, such scenario is also observed in carbon doped ZnO [16], boron doped ZnO [18], AlN [25] and CdS [30] systems. The Fermi level is, between the majority-spin and minority-spin states, near the top of the valence bands, indicating this system is a p-type ferromagnetic semiconductor.

To gain insight into the magnetic coupling mechanism between the boron dopants, we substitute double selenium atoms by two boron atoms in 64-atom supercell and construct three doped configurations based on the order of boron–boron separation. The expressions (0, $n$) denote the doped boron atoms pairs (Fig. 1). The geometry optimizations show the distances between

the two doped boron atoms extend a little except the (0, 1) doped configuration. The distances between the doped two boron atoms in (0, 2) and (0, 3) doped configurations extend from 5.668 to 5.692 Å and 6.941 to 7.097 Å, respectively. For the (0, 1) doped configuration, the two boron atoms share the same zinc atom. The geometry optimization shows the distance between the two doped boron atoms shortens to 2.783 from 4.00 Å, and the angle formed by the B–Zn–B reduces to 79.5° from 108.5°.

In order to elucidate the stability of the ferromagnetic state with respect to the antiferromagnetic state, spin-polarized calculations are performed for the parallel (ferromagnetic) and antiparallel (antiferromagnetic phase) arrangement of spin on the boron atoms. The energy of ferromagnetic and antiferromagnetic phases for the above doped configurations is calculated, respectively. Calculation shows no clear spin-splitting in the (0, 1) doped configuration, indicating boron in such doped configuration cannot induce the magnetism, which is mainly due to the distance between the two doped boron atoms 2.783 Å is too small, wherein the two boron atoms form the stable covalent bond and nonmagnetic state, which is similar to the carbon doped $TiO_2$ [22] and ZnO [31]. While spin polarization ferromagnetic and antiferromagnetic state calculations show both (0, 2) and (0, 3) doped configurations favor the ferromagnetic ground states, in which the energy of the antiferromagnetic states are higher than that of the ferromagnetic states by 26.32 and 56.26 meV, respectively, denoting the ferromagnetic coupling exists between the doped boron atoms in ZnSe host. Such large energy difference between the ferromagnetic and antiferromagnetic states for the (0, 3) doped configurations implies that the room temperature ferromagnetism for boron doped ZnSe is expected. Furthermore, the spin polarization energy for the (0, 1) doped configuration is 0.816 eV higher than that of (0, 2) doped configurations, meanwhile it is 1.033 eV higher than that of (0, 3) doped configurations, indicating the doped boron atoms have no clustering tendency in the ZnSe system.

Although the origin of the ferromagnetism in DMSs is still under controversies, several models, such as superexchange, double exchange, p–d hybridization exchange, bound magnetic polarons model, phenomenological Zener/Ruderman–Kittel–Kasuya–Yoshida, and spin–split donor impurity model have been proposed to illustrate the ferromagnetic exchange mechanism of the TMs-doped DMSs [32–35]. Our calculations show the ferromagnetism for boron doped ZnSe could be attributed to the carrier mediated ferromagnetic interaction. Electronic structures (Fig. 3) show the holes introduced by the doped boron atoms are the main carriers. For the hole-mediated ferromagnetism, the positions of the impurity bands determine the ferromagnetism mechanism. If the impurity states locate in the band gap, the double exchange interaction can be used to explain the ferromagnetism. That is, given the incomplete filling of bands, when the exchange splitting is bigger than the bandwidth, the ferromagnetic state is more stable than the antiferromagnetic state if a larger (usually rather small) number of holes (or electrons) exist. The band structures of boron doped ZnSe show the impurity bands are located in the band gap. The exchange splitting is bigger than the valence band (Fig. 3). The shallow acceptor levels indicate there are a considerable number of holes in such doped system. Therefore, the hole-mediated double exchange could be used to explain the ferromagnetism of the boron-doped ZnSe. The spin splitting for boron doped ZnSe is larger than that of the carbon doped ZnO [16], the room temperature ferromagnetism for carbon doped ZnO has been detected, which indicates boron doped ZnSe could be room temperature ferromagnetism.

To discuss the favorable doped configuration, the formation energy for the four high-symmetry cases including the above mentioned two substitutional ($B_{Se}$, $B_{Zn}$) and two interstitial $B_{iSe}$ and $B_{iZn}$ doped configurations are calculated, respectively. The formation energy of the defective system comprising of defects $\alpha$ is expressed as follows [36]:

$$E^f = E_D - E_H + \sum n_\alpha \mu_\alpha$$

where $E_D$ and $E_H$ are the energy of a system with and without defects. The $n_\alpha$ is the number of atoms removed (+) or added (-) to the host. The $\mu_\alpha$ is the chemical potential, which depends on the material grown conditions and satisfies boundary conditions. We employ the same method as Ref. [36] and use the energy of an atom in their crystal structure [37–39] to represent the chemical potential of zinc, boron and selenium, respectively. The formation energies for the $B_{Se}$, $B_{Zn}$, $B_{iZn}$ and $B_{iSe}$ doped configurations are 3.83, 2.82, 2.87 and 3.36 eV, which is mainly due to the ion radius of boron being much smaller than that of selenium. The formation energy indicates the boron prefer to form the $B_{Zn}$ and $B_{iZn}$ doped configurations by using the equilibrium method. However, the middle formation energy for $B_{Se}$ doped configuration indicates such doped case could be realized by using the nonequilibrium fabrication method.

## 4. Conclusions

We use the FPLAPW method with GGA and calculate the magnetism and electronic structure for the boron doped ZnSe. Our calculations show only boron substituting selenium could produce magnetism. Boron in substituting selenium doped configuration has spin-polarized B-2p orbitals in the band gap generating a magnetic moment of 0.89 $\mu_B$/B. The long ferromagnetic exchange exists in the doped boron atoms. Electronic structures show the holes mediated double exchange mechanism plays a key role in yielding the ferromagnetism of $B_{Se}$ doped configuration, and $B_{Se}$ is a p-type ferromagnetic semiconductor, while $B_{Zn}$ doped configuration make ZnSe be a n-type semiconductor. Shallower acceptor and donor levels indicate boron-doped ZnSe is ionized easily at working temperatures. These results imply the boron doped ZnSe could be applied in spintronics devices. We expect further experiments researches on boron-doped ZnSe.

## Acknowledgments

This work was supported by National Natural Science Foundation of China (Grant nos. 11174179 and 11074081). This work was also supported by the Yichang Science and Technology Project A2011-302-27 and the China Three Gorges University Project KJ2010B013.

## References

[1] S.A. Wolf, D.D. Awschalom, R.A. Buhrman, J.M. Daughton, S. von Molnár, M.L. Roukes, A.Y. Chtchelkanova, D.M. Treger, Science 294 (2001) 1488.
[2] S.G. Yang, A.B. Pakhomov, S.T. Hung, C.Y. Wong, Appl. Phys. Lett. 81 (2002) 2418.
[3] Y. Niwayama, H. Kura, T. Sato, M. Takahashi, T. Ogawa, Appl. Phys. Lett. 92 (2008) 202502.
[4] T.C. Kaspar, T. Droubay, V. Shutthanandan, S.M. Heald, C.M. Wang, D.E. McCready, S. Thevuthasan, J.D. Bryan, D.R. Gamelin, A.J. Kellock, M.F. Toney, X. Hong, C.H. Ahn, Phys. Rev. B 73 (2006) 155327.
[5] N.H. Hong, J. Sakai, A. Hassini, Appl. Phys. Lett. 84 (2004) 2602.
[6] A. Gupta, H. Cao, K. Parekh, K.V. Rao, A.R. Raju, U.V. Waghmare, J. Appl. Phys. 101 (2007) 09N513.
[7] C. Liu, F. Yun, H. Morko, J. Mater. Sci. Mater. Electron. 16 (2005) 555.
[8] G. Shao, J. Phys. Chem. C. 112 (2008) 18677.
[9] Z.Z. Zhang, B. Partoens, Kai Chang, F.M. Peeters, Phys. Rev. B **77** (2008) 155201.
[10] Y. Uspenskiia, E. Kulatov, H. Mariette, H. Nakayama, H. Ohta, J. Magn. Magn. Mater. 258 (2003) 248.

[11] A. Ney, K. Ollefs, S. Ye, T. Kammermeier, V. Ney, T.C. Kaspar, S.A. Chambers, F. Wilhelm, A. Rogalev, Phys. Rev. Lett. 100 (2008) 157201.
[12] S.A. Chambers, T. Droubay, C.M. Wang, A.S. Lea, R.F.C. Farrow, L. Folks, V. Deline, S. Anders, Appl. Phys. Lett. 82 (2003) 1257.
[13] S. Dhar, O. Brandt, A. Trampert, L. Däweritz, K.J. Friedland, K.H. Ploog, J. Keller, B. Beschoten, G. Güntherodt, Appl. Phys. Lett. 82 (2003) 2077.
[14] J.H. Park, M.G. Kim, H.M. Jang, S. Ryu, Y.M. Kim, Appl. Phys. Lett. 84 (2004) 1338.
[15] S. Zhou, Q. Xu, K. Potzger, G. Talut, R. Grötzschel, J. Fassbender, M. Vinnichenko, Jörg Grenzer, M. Helm, H. Hochmuth, M. Lorenz, M. Grundmann, H. Schmidt, Appl. Phys. Lett. 93 (2008) 232507.
[16] H. Pan, J.B. Yi, L. Shen, R.Q. Wu, J.H. Yang, J.Y. Lin, Y.P. Feng, J. Ding, L.H. Van, J.H. Yin, Phys. Rev. Lett. 99 (2007) 127201.
[17] K.B. Ruan, H.W. Ho, R.A. Khan, P. Rena, W.D. Song, A.C.H. Huan, L. Wang, Phys. Lett. A 150 (2010) 2158.
[18] X.G. Xu, H.L. Yang, Y. Wu, D.L. Zhang, S.Z. Wu, J. Miao, Y. Jiang, X.B. Qin, X.Z. Cao, B.Y. Wang, Appl. Phys. Lett. 97 (2010) 232502.
[19] H. Pan, Y.P. Feng, Q.Y. Wu, Z.G. Huang, J.Y. Lin, Phys. Rev. B **77** (2008) 125211.
[20] S.W. Fan, K.L. Yao, Z.L. Liu, Appl. Phys. Lett. 94 (2009) 152506.
[21] R. Long, Nialln.J. English, Phys. Rev. B 80 (2009) 115212.
[22] K.S. Yang, Y. Dai, B.B. Huang, M.H. Whangbo, Appl. Phys. Lett. 93 (2008) 132507.
[23] X.F. Wang, X.S. Chen, H.B. Shu, R.B. Dong, Y. Huang, W. Lu, Solid State Commun. 149 (2009) 1717.
[24] L. Shen, R.Q. Wu, H. Pan, G.W. Peng, M. Yang, Z.D. Sha, Y.P. Feng, Phys. Rev. B 78 (2008) 073306.
[25] X. Peng, R. Ahuja, Appl. Phys. Lett. 94 (2009) 102504.
[26] K. Schwarz, P. Blaha, G.K.H. Madsen, Comput. Phys. Commun. 147 (2002) 71.
[27] J.P. Perdew, K. Burke, M. Ernzerhof, Phys. Rev. Lett. 77 (1996) 3865.
[28] N. Kh., V.B. Abrikosov, L.V. Bankina, L.E. Poretskaya, Shelimova, E.V. Skudnova, Semiconducting II-VI, IV-VI, and V-VI Compounds, Plenum, New York, 1969, p. 2.
[29] 〈http://www.webelements.com〉.
[30] Y.D. Ma, Y. Dai, B.B. Huang, Comput. Mater. Sci. 50 (2011) 1661.
[31] B.J. Nagare, S. Chacko, D.G. Kanhere, J. Phys. Chem. A. 114 (2010) 2689.
[32] H. Akai, Phys. Rev. Lett. 81 (1998) 3002.
[33] A. Kaminski, S. Das Sarma, Phys. Rev. Lett. 88 (2002) 247202.
[34] Y.J. Zhao, T. Shishidou, A.J. Freeman, Phys. Rev. Lett. 90 (2003) 047204.
[35] J.M.D. Coey, M. Venkatesan, C.B. Fitzgerald, Nature Mater. 4 (2005) 173.
[36] X.Y. Cui, B. Delley, A.J. Freeman, C. Stampfl, Phys. Rev. B 76 (2007) 045201.
[37] A.W. Hull, W.P. Davey, Phys. Rev. 17 (1921) 549.
[38] B.F. Decker, J.S. Kasper, Acta Crystallogr. 12 (1959) 503.
[39] Y. Miyamoto, Jpn. J. Appl. Phys. 19 (1980) 1813.